

On the roles of sparsity and sparsifying transforms in Computerized Tomography

Indian Institute of Technology, Hyderabad

Department of Mathematics

Report of M.Sc Project

MUNNU SONKAR



भारतीय प्रौद्योगिकी संस्थान हैदराबाद
Indian Institute of Technology Hyderabad

SUPERVISOR : DR. C. S. SASTRY

DECLARATION

I declare that this written submission represents my ideas in my own words and where others' ideas or words have been included, I have adequately cited and referenced the original sources. I also declare that I have adhered to all principles of academic honesty and integrity and have not misrepresented any idea in my submission. I understand that any violation of the above will be cause for disciplinary action by the Institute and can also evoke penal action from the source which have thus not been properly cited or from whom proper permission has not been taken when needed.

C. S. CASTRY

(Signature of the supervisor)

C. S. CASTRY

(Name of the supervisor)

MUNNU SONKAR

(Signature of the student)

MUNNU SONKAR

(Name of the student)

MA13M1005

(Roll no)

Date: 4-MAY-2015

Place: IIT HYDERABAD

APPROVAL SHEET

This thesis entitled "**On the roles of sparsity and sparsifying transforms in Computerized Tomography**" by MUNNU SONKAR is approved for the degree of MASTER OF SCIENCE.

C.C. CASTRY

(Signature of the supervisor)

(C.C. CASTRY)

(Name of the supervisor)

Date: 4/MAY/2015

Place: IIT HYDERABAD

Abstract

X-ray computed tomography (CT) is one of the most widely used imaging modalities for diagnostic tasks in the clinical application. As X-ray dosage given to the patient has potential to induce undesirable clinical consequences, there is a need for reduction in dosage while maintaining good quality in reconstruction.

This report explores the roles of concept of sparsity and sparsifying transforms via Frames, Wavelets etc and their relevance to low-dose tomography. After giving detailed descriptions of basics of Computed Tomography, Frames/Wavelets and Compressive Sensing Theory, the report proposes a TV-norm based method for the reconstruction of Tomography. Finally, the report ends with some discussion on simulation results.

Contents

1	Introduction to Computerized Tomography	3
1.1	History	3
1.2	X ray CT	4
1.2.1	“Standard” X-ray CT:	4
1.3	Beer’s law and the X-ray/Radon transforms	4
1.3.1	Beer’s law	5
1.3.2	X-ray and Radon transforms	6
1.3.3	Parameterization of X-ray transform	6
1.3.4	Sinograms	8
1.4	Properties of X-ray(=Radon) transform in two dimensions	8
1.4.1	Shift invariance	9
1.4.2	Rotation invariance	10
1.4.3	Dilation invariance	10
1.4.4	Relation with the Fourier transform: Projection- theorem	11
1.4.5	X-ray transform as a mapping between function spaces	11
1.5	Backprojection	13
1.6	Inversion	13
2	Compressed Sensing	15
2.1	Introduction	15
2.2	Mathematics of Compressed Sensing	16
2.3	Greedy Methods	16
2.3.1	Orthogonal Matching Pursuite	17

2.4	Convex optimization technique:	18
3	Introduction to frames	20
3.1	Some basic facts about frames	20
3.2	Pseudo inverses	27
3.3	Singular value decomposition	30
4	Wavelet Analysis	32
4.1	Discrete Wavelet Transform	32
4.2	Wavelet tight frame in 1D	34
5	Computed Tomography in Compressive Sensing Framework	37
5.1	Algebraic Reconstruction Technique (ART)	37
5.2	1D TV Optimization	39
6	Experimental Result	43

Chapter 1

Introduction to Computerized Tomography

1.1 History

In the standard X-ray picture procedure, the X-rays from a source pass through the patient's body and leave a trace on the film. Therefore, the resulting X-ray picture is essentially the overlap of images of all s (parallel to the film) of body. This makes reading X-ray pictures an art and requires a lot of training. Even trained professionals might not be able to detect a small tumor hiding behind a dense bone. Almost a hundred years ago, doctors came up with a smart idea (now called "old" or traditional tomography). One of its versions involves moving the source with a constant speed parallel to the film and simultaneously moving the film in the opposite direction with coordinated constant speed. A simple planar geometry consideration (Fig 1.1) shows that there is single s /layer parallel to the film which is projected on to the same location of the film and thus sharpened, while the images of all s will move and thus get blurred. Hence, this simple technique sharpens the image of a chosen layer while blurring the rest of them. However, the blurred remnants of uninteresting layers are still present and still cause problems while reading X-ray pictures.

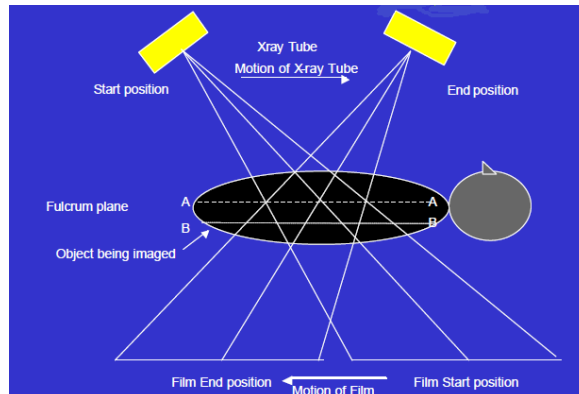


Figure 1.1: Old tomography

1.2 X ray CT

1.2.1 “Standard” X-ray CT:

A very narrow (“pencil”) beam of X-rays is sent through patient’s body. The original intensity of the beam is known, and a detector finds the outgoing intensity at beam’s exit. The exit intensity is lower than the original one, due to photon being absorbed and scattering inside of the body. So, one collects the two numbers initial and terminal intensities. Then the direction of beam is changed, and a new a pairs of numbers collected. This procedure is repeated for large number of rays, which provides a large amount of data. Since the rate of weakening of the beam depends on the type of tissue it passes through, there is hope of recovering the internal structure of the body from the collected data.

1.3 Beer’s law and the X-ray/Radon trans- forms

Now we are going to develop a mathematical model of data collected by an X-ray CT scanner.

1.3.1 Beer's law

Let a pencil beam l be just a line. Suppose the initial intensity of beam is I_0 , terminal intensity is I_1 and $I(x)$ is the intensity of the beam l at a location x , then Beer's law state -the infinitesimal relative drop of intensity at distance Δx from the location x should be proportional to the distance traveled. i.e.,

$$\frac{\Delta I}{I} \propto \Delta x$$

$$\frac{\Delta I}{I} = -\mu(x) \Delta x,$$

where $\mu(x)$ is the attenuation coefficient of the tissue at the point x .

Now above equation gives us

$$\frac{d}{dx}(I) = -\mu(x)I$$

$$\frac{dI}{I} = -\mu(x)dx$$

$$\log(I) = \int -\mu(x)dx + C.$$

Given that, at $x=0, I = I_0$ we have,

$$\log(I_0) = C.$$

Substituting the value of C we get,

$$\log\left(\frac{I}{I_0}\right) = \int -\mu(x)dx.$$

After traversing the line l the intensity at the detector is I_1 , then

$$\int_l \mu(x) d(x) = \log \frac{I_0}{I_1}.$$

1.3.2 X-ray and Radon transforms

Definition 1.3.1. Let $f(X) = f(x, y)$ be the compactly supported and continuous function on \mathbf{R}^2 . The X-ray(Radon) transform Rf is a function defined on the space of straight lines (l) in \mathbf{R}^2 by the line integral along each such line.

$$Rf(l) = \int_l f(X) d(s).$$

where ds is the arc length measure along the line l .

Remark 1.3.2. Radon transform in 2D is X-ray transform.

1.3.3 Parameterization of X-ray transform

In order to work in the circular geometry of CT scans, it is helpful to parametrize lines $ax + by = c$ in R^2 to a set of oriented lines with radial parameters 't' in $R \times S^1$. In medical imaging, these lines are representative of the trajectories of X-ray beams entering a body. Consider the general line in R^2

$$ax + by = c, \tag{a}$$

where a, b, and c are constants. we have

$$\frac{a}{\sqrt{(a^2 + b^2)}}x + \frac{b}{\sqrt{(a^2 + b^2)}}y = \frac{c}{\sqrt{(a^2 + b^2)}}.$$

the first two coefficients, $(\frac{a}{\sqrt{a^2+b^2}}, \frac{b}{\sqrt{a^2+b^2}})$, define a point on the unit circle. Let θ be the angle corresponding to that point on the unit circle, so $\theta = \cos^{-1}(\frac{a}{\sqrt{a^2+b^2}})$ then $\cos \theta = \frac{a}{\sqrt{a^2+b^2}}$ and $\sin \theta = \frac{b}{\sqrt{a^2+b^2}}$. The angle θ can only take on values of $[0; \pi)$ before repeating previously described lines. Let t be the distance from the origin to the line $ax+by = c$ along the angle θ . Then the line can also be described as the set of solutions (x, y) to the inner-product

$$t = \langle (x, y), (\cos \theta, \sin \theta) \rangle = \langle (x, y), w \rangle.$$

Therefore, t is equal to the right side of equation (a). Notice that our definitions of t and θ also give us a point on the line, $(t \cos \theta; t \sin \theta)$, where a line at angle θ intersects $ax + by = c$. This intersection is a right angle, because while the slope of the line $ax + by = c$ is $-\frac{a}{b}$, the tangent of θ is

$$\tan \theta = \frac{\sin \theta}{\cos \theta} = \frac{b}{a}.$$

Let the vector $\omega = \langle \cos \theta, \sin \theta \rangle$ perpendicular to the line $ax + by = c$, and let the vector $\omega^\perp = \langle -\sin \theta, \cos \theta \rangle$ be perpendicular to this line. We can therefore create a vector equation in terms of t and θ for the line,

$$l_{t,\theta} = t\omega + s\omega^\perp$$

$$l_{t,\theta} = t\langle \cos \theta, \sin \theta \rangle + s\langle -\sin \theta, \cos \theta \rangle,$$

where s in \mathbf{R} .

Definition 1.3.3. Let f be some function in \mathbf{R}^2 , parametrized over the lines $l_{t,\theta}$. The Radon transform $Rf(t;\omega)$ is defined as

$$Rf(t;\omega) = g(t,\omega) = \int_{x.\omega=t} f ds = \int_{-\infty}^{\infty} f(t\omega + s\omega^\perp) ds = \int_{-\infty}^{\infty} f(t \cos \theta - s \sin \theta, t \sin \theta + s \cos \theta) ds.$$

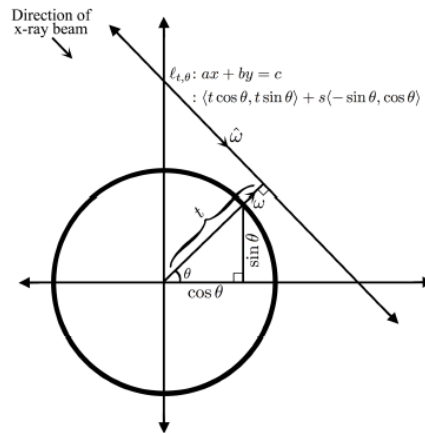


Figure 1.2: Parametric representation of line $ax + by = c$

1.3.4 Sinograms

A **sinogram** is the density plot of the X-ray transform of 2D function.

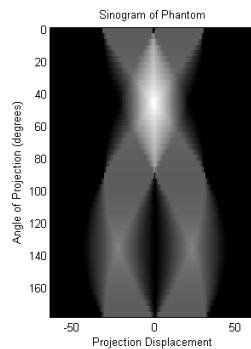


Figure 1.3: Sinogram(density plot of the X-ray transform)

1.4 Properties of X-ray(=Radon) transform in two dimensions

Now we are going to explore some properties of Radon transform [1].

1.4.1 Shift invariance

Let $a \in \mathbb{R}^2$ and let $T_a f(x) := f(x + a)$ be the corresponding shift operator acting on the function on the plane. Analogously, $T_s g(t, \omega) := g(t + s, \omega)$ is the (axial) shift on the cylinder \mathbb{T} .

Proposition 1.4.1. *The following commutation relation holds:*

$$R(T_a f)(t, \omega) = (T_{a, \omega} R)f(t, \omega).$$

Proof- We know that

$$Rf(t) = \int_{x, \omega=t} f(x) ds$$

so

$$R(T_a f)(t, \omega) = \int_{x, \omega=t} T_a(f) ds$$

$$R(T_a f)(t, \omega) = \int_{x, \omega=t} f(x + a) dx$$

$$\text{put } \rightarrow y = x + a, \implies dy = dx,$$

and

$$y, \omega = t + a, \omega$$

$$R(T_a f)(t, \omega) = \int_{y, \omega=t+a, \omega} f(y) dy$$

$$R(T_a f)(t, \omega) = g(t + a, \omega, \omega)$$

$$R(T_a f)(t, \omega) = T_s g(t, \omega)$$

$$R(T_a f)(t, \omega) = (T_{a, \omega} R) f(t, \omega).$$

1.4.2 Rotation invariance

Let A be 2×2 rotation matrix, $M_A f(x) := f(Ax)$ be the corresponding rotation operator and corresponding rotation operator on \mathbb{T} , $T : M_A g(t, \omega) := g(t, A\omega)$

Proposition 1.4.2. *The following commutation relation holds for any rotation matrix A ;*

$$RM_A = M_A R.$$

This property, has a simple geometric meaning; instead of integrating a function over a rotated line .we can integrate the appropriately rotated function along the original line.

1.4.3 Dilation invariance

Let $r > 0$ be a positive number, and D_r the radial dilation operator $D_r f(x) := f(rx)$. An analogous operator acts on functions on the cylinder $T : D_r g(t, \omega) := g(rt, \omega)$.

Proposition 1.4.3. *The following commutation relation holds:*

$$RD_r = \frac{1}{r} D_r R$$

1.4.4 Relation with the Fourier transform: Projection-theorem

The next statement (called the projection-, Fourier-, or central formula) is indeed central for studying the X-ray and Radon transforms.

Theorem 1.4.4. *Under appropriate conditions on a function $f(x)$ on \mathbb{R}^2 the following relation holds:*

$$\hat{R}f(\sigma, \omega) = \tilde{f}(\sigma\omega).$$

Proof.

$$\begin{aligned} \hat{R}f(\sigma, \omega) &= \int g(t, \omega) e^{-i\sigma t} dt \\ &= \int_{\mathbb{R}} \int_{-\infty}^{\infty} f(t\omega + s\omega^\perp) ds e^{-i\sigma t} dt \\ &= \int_{\mathbb{R}^2} f(x) e^{-i\sigma x \cdot \omega} dx \\ &= \tilde{f}(\sigma\omega). \end{aligned}$$

□

Fourier- theorem says that taking a 1D Fourier transform of Radon transform Rf of f on the plane, one recovers the 2D Fourier transform of f .

1.4.5 X-ray transform as a mapping between function spaces

Consider the weighted spaces $L_2([-1, 1] \times S^1, (1 - t^2)^{-\frac{1}{2}})$ that consists of functions on the finite cylinder $[-1, 1] \times S^1$ having finite weighted L_2 -norm,

$$\int_{-1}^1 \int_S |g(t, \omega)|^2 \frac{d\omega dt}{\sqrt{1 - t^2}}.$$

We denote, Ω as unit disk in \mathbb{R}^2 centered at the origin and assume that the function is supported inside Ω .

Theorem 1.4.5. *The Radon transform R is a continuous linear operator from $L_2(\Omega)$ to $L_2([-1, 1] \times S^1, (1 - t^2)^{-\frac{1}{2}})$.*

Proof. Consider a function $f \in L_2(\Omega)$ (ie., it is square integrable and supported in unit the disk).then

$$\|Rf(t, \omega)\|^2 = \|g(t, \omega)\|^2 = \int_{-1}^1 \int_s^1 |g(t, \omega)|^2 \frac{dwdt}{\sqrt{1-t^2}}.$$

where $|g(t, \omega)| = \left| \int_{-\sqrt{1-t^2}}^{\sqrt{1-t^2}} f(t\omega + s \perp \omega) ds \right|$. Now, we will compute first $|g(t, \omega)|^2 \frac{1}{\sqrt{1-t^2}}$.

Consider the function

$$\chi(s) = \begin{cases} 1 & \text{when } |s| \leq \sqrt{1-t^2}, \\ 0 & \text{otherwise.} \end{cases}$$

then

$$\left| \int_{-\sqrt{1-t^2}}^{\sqrt{1-t^2}} f(t\omega + s\omega^\perp) ds \right| = \int_{-\infty}^{\infty} \chi(s) f(t\omega + s\omega^\perp) ds$$

thus by Cauchy-Schwarz inequality-

$$\frac{|g(t, \omega)|^2}{\sqrt{1-t^2}} \leq 2 \int_{-\infty}^{\infty} |f(t\omega + s\omega^\perp)|^2 ds,$$

here, $\{2 \int_{-\infty}^{\infty} |f(t\omega + s\omega^\perp)|^2 ds\}$ is finite.

thus,

$$\|g\|^2 = \int_{-1}^1 \int_s^1 |g(t, \omega)|^2 \frac{dwdt}{\sqrt{1-t^2}}$$

is bounded. So

$\|g\|$ is bounded, which implies that $g(t, \omega) = Rf(t, \omega)$ is continuous.

□

1.5 Backprojection

Backprojection is the dual operator $R^\# : L_2(T) \rightarrow L_2(\mathbb{R}^2)$ to $R : L_2(\mathbb{R}^2) \rightarrow L_2(T)$ i.e., such that

$$(Rf, g)_{L_2(T)} = (f, R^\#g)_{L_2(\mathbb{R}^2)}. \quad (1.1)$$

Proof.

$$\begin{aligned} (Rf, g)_{L_2(T)} &= \int_S d\omega \int_{-\infty}^{\infty} Rf(t, \omega)g(t, \omega)dt \\ &= \int_{S^1} d\omega \int_{-\infty}^{\infty} \left(\int_{x.\omega=t} f(x)dx \right) g(t, \omega)dt \\ &= \int_{S^1} d\omega \int_{\mathbb{R}^2} f(x)g(x.\omega, \omega)dx \\ &= \int_{\mathbb{R}^2} f(x) \left(\int_{S^1} g(x.\omega, \omega) \right) dx. \\ R^\#g(x) &= \int_{S^1} g(x.\omega, \omega) d\omega. \end{aligned}$$

□

Geometrically, to get the value of $R^\#g$ at a point x , choose a line through x , which implies that the parameter of this line are $(x.\omega, \omega)$; and then averages over all lines through x .

As the result, one gets a web of lines, the density of which can be understood as $R^\#g$. In other words, a single point source will produce the overlap of a bunch of lines passing through it. A calculation shows that this the same as saying that $R^\#\delta = \frac{2}{|x|}$, where $\delta(s)$ is delta-function. And thus instead of the sharp δ – *pick*, one gets its blurred version $\frac{2}{|x|}$

1.6 Inversion

An explicit inversion formula can be obtained by using the projection Formula and Fourier inversion formula. Indeed, passing from Cartesian coordinate to

the polar ones (σ, ω) (where $\xi = \sigma\omega$), we obtain

$$\begin{aligned}
f(x) &= \frac{1}{(2\pi)^2} \int_{\mathbb{R}^2} \tilde{f}(\xi) e^{ix \cdot \xi} d\xi \\
&= \frac{1}{(2\pi)^2} \int_{S^1} \int_0^\infty \tilde{f}(\sigma\omega) e^{i\sigma x \cdot \omega} \sigma d\sigma d\omega \\
&= \frac{1}{2} \frac{1}{(2\pi)^2} \int_{S^1} \int_{-\infty}^\infty \tilde{f}(\sigma\omega) e^{i\sigma x \cdot \omega} |\sigma| d\sigma d\omega
\end{aligned}$$

where we used $\tilde{f}((- \sigma)(\omega)) = \tilde{f}(\sigma\omega)$.

Finally, we have the following reconstruction formula

$$f(x) = \frac{1}{2} \frac{1}{(2\pi)^2} \int_{S^1} \int_{-\infty}^\infty \hat{g}(\sigma, \omega) e^{i\sigma x \cdot \omega} |\sigma| d\sigma d\omega$$

Chapter 2

Compressed Sensing

2.1 Introduction

In signal and image processing, one would like to reconstruct a signal from measured data. When the information acquisition process is linear, the problem reduces to solving a linear system of equations. In mathematical terms, the observed data $y \in \mathbb{R}^m$ is connected to the signal $x \in \mathbb{R}^M$ of interest via

$$y = \Phi x. \tag{2.1}$$

The matrix $\Phi \in \mathbb{R}^{m \times M}$ models the linear measurement process (referred conventionally to as dictionary), the vector $y \in \mathbb{R}^m$ is the measurement vector. Then one tries to recover the vector $x \in \mathbb{R}^M$ by solving the above linear system. When the number of measurements m is equal to M , the recovered x is in general $\Phi^{-1}y$. However, in many applications, it is much more desirable to take fewer measurements, provided one can still recover the signal. In particular, when $m < M$, the linear system $\Phi x = y$ is typically underdetermined and in general it has infinitely many solutions. In this case, an interesting question arises: “is it still possible to recover x possessing fewer nonzero components from y through a computationally tractable procedure?” The research direction that deals with this problem has become popular as Compressive Sensing (CS), Compressed Sensing (CS), Compressive Sampling, or Sparse Representations.

Denoting Φ_k^r as the k^{th} row of Φ , one may rewrite the k^{th} component in y as $y_k = \langle \Phi_k^r, x \rangle$, $k = 1, 2, \dots, m$. Here $\langle \Phi_k^r, x \rangle$ represents the inner-product between Φ_k^r and x . That is, the object x to be acquired is correlated with the waveform Φ_k^r . This is a standard setup in several applications. For example, if the sensing waveforms are Dirac delta functions, then y is a vector of sampled values of x in time or space domain. If the sensing waveforms are indicator functions of pixels, then y is the image data typically collected by sensors in a digital camera. If the sensing waveforms are sinusoids, then y is a vector of Fourier coefficients and this modality is used in the Magnetic Resonance Imaging (MRI). Nevertheless, if the sensing waveforms have 0 and 1 (or 0 and ± 1) as elements, then the associated matrix (referred conventionally to as a sensing matrix) can have potential applications for multiplier-less dimensionality reduction.

2.2 Mathematics of Compressed Sensing

A vector $x \in \mathbb{R}^M$ is k -sparse if it has at most k nonzero coordinates. That is, $\|x\|_0 := |\{i \mid x_i \neq 0\}| = k < M$. One can recover the sparse x from its linear measurements by solving the following optimization problem:

$$P_0 : \min_{\alpha} \|\alpha\|_0 \text{ subject to } \Phi\alpha = y. \quad (2.2)$$

The l_0 -minimization problem in (2.2) is in general NP-hard. There are two classes of methods, namely Greedy and Convex optimization technique used for solving (2.2)

2.3 Greedy Methods

These methods iteratively approximate the coefficients and the support of the original signal, which enjoy the advantage of faster implementation. Among the existing greedy methods, the most popular one is orthogonal matching pursuit (OMP).

2.3.1 Orthogonal Matching Pursuite

One can obtain k sparse approximation in k steps (that is one column per one step). The j -th test can be done by minimizing $\epsilon(j) = \|\phi_j z_j - b\|_2$, leading to $z_j^* = \frac{\phi_j^T b}{\|\phi_j\|_2^2}$. The associated error has the following expression

$$\begin{aligned}\epsilon(j) &= \|\phi_j z_j - b\|_2^2 = \left\| \frac{\phi_j^T b}{\|\phi_j\|_2^2} \phi_j - b \right\|_2^2 \\ &= \|b\|_2^2 - 2 \frac{(\phi_j^T b)^2}{\|\phi_j\|_2^2} + \frac{(\phi_j^T b)^2}{\|\phi_j\|_2^2} \\ &= \|b\|_2^2 - \frac{(\phi_j^T b)^2}{\|\phi_j\|_2^2}.\end{aligned}$$

If this error is zero, One obtains proper solution. Thus the test to be done is simply $\|\phi\|_2^2 \|b\|_2^2 = (\phi_j^T b)^2$ which indicates that b and a_j are parallel.

A greedy strategy abandons exhaustive search in favor of a series of locally optimal single-term updates. Starting from $x^0 = 0$ it iteratively constructs a k -term approximant x^k by maintaining a set of active columns expanding that set by one additional column. The column chosen at each stage maximally reduces the residual l_2 error in approximating b from the currently active columns. After constructing an approximant including the new column, the residual l_2 error is evaluated; if it now falls below a specified threshold, the algorithm terminates.

Task: Approximate the solution of $P_0 : \min_x \|x\|_0$ subject to $\Phi x = y$.

Input: Φ , b , ϵ_0 (error threshold).

Initialization: Initialize $k = 0$, and set

- The initial solution $x^0 = 0$.
- The initial residual $r^0 = b - \Phi x^0 = b$.
- The initial solution support $S^0 = \text{Support}\{x^0\} = \emptyset$.

Main Iteration: Increment k by 1 and perform the following steps:

- **Sweep:** Compute the errors $\epsilon(j) = \min_{z_j} \|\phi_j z_j - r^{k-1}\|_2^2$ for all j using the optimal choice $z_j^* = \frac{\phi_j^T r^{k-1}}{\|\phi_j\|_2^2}$.
 - **Update Support:** Find a minimizer j_0 of $\epsilon(j) : \forall j \notin S^{k-1}, \epsilon(j_0) \leq \epsilon(j)$, and update $S^k = S^{k-1} \cup \{j_0\}$.
 - **Update Provisional Solution:** Compute x^k , the minimizer of $\|\Phi x - \mathbf{b}\|_2^2$ subject to $\text{support}\{x\} = S^k$
 - **Update Residual:** Compute $r^k = \mathbf{b} - \Phi x^k$.
 - **Stopping Rule:** If $\|r^k\|_2 < \epsilon_0$, stop. Otherwise, apply another iteration.
- Output:** The proposed solution is x^k obtained after k iterations.

2.4 Convex optimization technique:

The second class of methods, called convex optimization methods, consider the convex relation of $\|\cdot\|_0$ -norm in (p_0) and reposes the problem as

$$P_1 : \min_x \|x\|_1 \quad \text{subject to} \quad \Phi x = y. \quad (2.3)$$

A sufficient condition for the equivalence of p_0 and p_1 problems is given by the Restricted Isometry Property

Definition 2.4.1. *An $m \times M$ matrix Φ is said to satisfy the Restricted Isometry Property (RIP) of order k with constant δ_k ($0 < \delta_k < 1$) if for all vectors $x \in \mathbb{R}^M$ with $\|x\|_0 \leq k$, we have*

$$(1 - \delta_k) \|x\|_2^2 \leq \|\Phi x\|_2^2 \leq (1 + \delta_k) \|x\|_2^2. \quad (2.4)$$

To get a better understanding of this property, consider the $m \times |T|$ matrices Φ_T formed by the columns of Φ with indices from $T \subset \{1, 2, \dots, M\}$. Then (2.4) is equivalent to showing that the Grammian matrices $A_T := \Phi_T^t \Phi_T, |T| \leq k$ have their eigenvalues in $[1 - \delta_k, 1 + \delta_k]$. The following proposition relates the RIP constant δ_k and μ .

Proposition 2.4.2. *Suppose that ϕ_1, \dots, ϕ_M are the unit norm columns of the matrix Φ with coherence μ . Then Φ satisfies RIP of order k with constant $\delta_k = (k - 1)\mu$.*

Chapter 3

Introduction to frames

Basis is one of the most important concept in a study of vector spaces which allows us to write each element in the vector space as the linear combination of the elements in the basis. But we have the extra condition that the elements of the basis need to be linearly independent. In fact, in the case of inner-product spaces, we look for those elements which are orthogonal to each other. This conditions make it harder to find a basis for a space which is why we look for some more general tools which can relax some conditions but work similar to that of a basis.

Frame for a vector space equipped with an inner-product also allows each element in the space to be written as a linear combination of the elements in the frame, In the thesis, we study mainly frames in finite dimensional inner-product spaces.

3.1 Some basic facts about frames

Let V be a finite dimensional vector space, equipped with an inner-product space $\langle \cdot, \cdot \rangle$, which we choose to be linear in the first entry. Recall that a sequence $\{e_k\}_{k=1}^m$ in V is a basis for V if the following two conditions are satisfied:

(i) $V = \text{span} \{e_k\}_{k=1}^m$;

(ii) $\{e_k\}_{k=1}^m$ is linearly independent; i.e., if $\sum_{k=1}^m c_k e_k = 0$ or some scalar coefficients $\{c_k\}_{k=1}^m$, then $c_k = 0$, $\forall k = 1, 2, \dots, m$;

As a result, every $f \in V$ has a unique representation in terms of the elements of the basis, i.e., there exists unique set of scalars $\{c_k\}_{k=1}^m$ such that

$$f = \sum_{k=1}^m c_k e_k. \quad (3.1)$$

If $\{e_k\}_{k=1}^m$ is an orthonormal basis, i.e., a basis for which

$$\langle e_k, e_j \rangle = \delta_{x,y} = \begin{cases} 1, & \text{if } k = j \\ 0, & \text{if } k \neq j, \end{cases}$$

then the coefficients $\{c_k\}_{k=1}^m$ are easy to find. Taking the inner-product of f in (1.1) with an arbitrary e_j gives

$$\langle f, e_j \rangle = \left\langle \sum_{k=1}^m c_k e_k, e_j \right\rangle = \sum_{k=1}^m c_k \langle e_k, e_j \rangle = c_j$$

or

$$f = \sum_{k=1}^m \langle f, e_k \rangle e_k. \quad (3.2)$$

We in this chapter, introduce the concept of frames which also allows a representation of vectors like (1.1) which we will prove.

Definition 3.1.1. *A countable family of elements $\{f_k\}_{k \in I}$ in V is a frame for V if there exist constants $A, B > 0$ such that*

$$A\|f\|^2 \leq \sum_{k \in I} |\langle f, f_k \rangle|^2 \leq B\|f\|^2, \quad \forall f \in V. \quad (3.3)$$

[2]

The numbers A, B are called frame bounds. They are not unique. The optimal lower frame bound is the supremum over all lower frame bounds,

and the optimal upper frame bound is the infimum over all upper frame bounds. Note that the optimal frame bounds are actually frame bounds. The frame is normalized if $\|f_k\| = 1, \quad \forall k \in I$. In a finite-dimensional vector space it is somehow artificial (though possible) to consider families $\{f_k\}_{k \in I}$ having infinitely many elements. In this project we consider finite families $\{f_k\}_{k=1}^m, \quad m \in \mathbb{N}$. With this restriction, Cauchy-Schwarz' inequality shows that

$$\sum_{k=1}^m |\langle f, f_k \rangle|^2 \leq \sum_{k=1}^m \|f_k\|^2 \|f\|^2, \quad \forall f \in V,$$

i.e. the upper frame condition is automatically satisfied. However, one can often find a better upper frame bound than $\sum_{k=1}^m \|f_k\|^2$. In order for the lower condition in (1.3) to be satisfied, it is necessary that $\text{span}\{f_k\}_{k=1}^m = V$. This condition turns out to be sufficient; in fact, every finite sequence is a frame for its span.

Proposition 3.1.2. *Let $\{f_k\}_{k=1}^m$ be a sequence in V . Then $\{f_k\}_{k=1}^m$ is a frame for $\text{span}\{f_k\}_{k=1}^m$.*

Proof. Assume that not all $\{f_k\}$ are zero.

The upper frame condition is automatically satisfied with $B = \sum_{k=1}^m \|f_k\|^2$. We have to find the lower bound A. Now Let

$$W = \text{span}\{f_k\}_{k=1}^m, \quad W' = \{f \in W : \|f\| = 1\}$$

and consider the mapping

$$\phi: W \rightarrow \mathbb{R}, \quad \phi(f) = \sum_{k=1}^m |\langle f, f_k \rangle|^2.$$

ϕ is a continuous function because it is the composition of continuous functions. Now, since W' is a compact set and ϕ is continuous function on it, ϕ attains its maximum and minimum on W' . i.e., we can find $g \in W$ with $\|g\| = 1$ such that

$$A = \sum_{k=1}^m |\langle g, f_k \rangle|^2 = \inf \left\{ \sum_{k=1}^m |\langle f, f_k \rangle|^2 : f \in W, \|f\| = 1 \right\}$$

Clearly $A > 0$ as it is sum of squares. Now, given $f \in W$, $f \neq 0$, we have

$$\sum_{k=1}^m |\langle f, f_k \rangle|^2 = \sum_{k=1}^m \left| \left\langle \frac{f}{\|f\|}, f_k \right\rangle \right|^2 \|f\|^2 \geq A \|f\|^2.$$

□

Corollary 3.1.3. *A family of elements $\{f_k\}_{k=1}^m$ in V is a frame for V if and only if $\text{span } \{f_k\}_{k=1}^m = V$.*

In particular, if $\{f_k\}_{k=1}^m$ is a frame for V and $\{g_k\}_{k=1}^n$ is an arbitrary finite collection of vectors in V , then $\{f_k\}_{k=1}^m \cup \{g_k\}_{k=1}^n$ is also a frame for V . A frame which is not a basis is said to be *overcomplete* or *redundant*.

Now consider a vector space V equipped with a frame $\{f_k\}_{k=1}^m$ and define a linear mapping

$$T: \mathbb{C}^m \rightarrow V, \quad T\{c_k\}_{k=1}^m = \sum_{k=1}^m c_k f_k. \quad (3.4)$$

T is usually called the *pre-frame operator*, or the *synthesis operator*. The *adjoint operator* is given by

$$T^*: V \rightarrow \mathbb{C}^m, \quad T^*\{f\} = \{\langle f, f_k \rangle_{k=1}^m\}, \quad (3.5)$$

and is called the *analysis operator*. By composing T with its adjoint T^* , we obtain the *frame operator*.

$$S: V \rightarrow V, \quad Sf = TT^*f = \sum_{k=1}^m \langle f, f_k \rangle f_k. \quad (3.6)$$

Now, in terms of the frame operator,

$$\langle Sf, f \rangle = \sum_{k=1}^m |\langle f, f_k \rangle|^2, \quad \forall f \in V. \quad (3.7)$$

the lower frame condition can thus be considered as some kind of "lower bound" on the frame operator.

A frame $\{f_k\}_{k=1}^m$ is called a *tight frame* if $A = B$, i.e., if

$$\sum_{k=1}^m |\langle f, f_k \rangle|^2 = A \|f\|^2, \quad \forall f \in V. \quad (3.8)$$

For a tight frame, the exact value A in (1.8) is simply called the frame bound.

Proposition 3.1.4. *Assume that $\{f_k\}_{k=1}^m$ is a tight frame for V with frame bound A . Then $S=AI$ (here I is the identity operator on V), and*

$$f = \frac{1}{A} \sum_{k=1}^m \langle f, f_k \rangle f_k, \quad \forall f \in V. \quad (3.9)$$

For general frames, we now prove that we still have a representation of each $f \in V$ of the form $f = \sum_{k=1}^m \langle f, g_k \rangle f_k$ for an appropriate choice of $\{g_k\}_{k=1}^m$. The second part of the following theorem, which is one of the important results in frames, is called the frame decomposition.

Theorem 3.1.5. *Let $\{f_k\}_{k=1}^m$ be a frame for V with frame operator S . Then*

(i) *S is invertible and self-adjoint.*

(ii) *Every $f \in V$ can be represented as*

$$f = \sum_{k=1}^m \langle f, S^{-1} f_k \rangle f_k = \sum_{k=1}^m \langle f, f_k \rangle S^{-1} f_k. \quad (3.10)$$

(iii) *If $f \in V$ also has the representation $f = \sum_{k=1}^m c_k f_k$ for some scalar coefficients $\{c_k\}_{k=1}^m$, then*

$$\sum_{k=1}^m |c_k|^2 = \sum_{k=1}^m |\langle f, S^{-1} f_k \rangle|^2 + \sum_{k=1}^m |c_k - \langle f, S^{-1} f_k \rangle|^2.$$

Proof. Since $S = TT^*$, $S = S^*$ which means that S is self-adjoint. We will now prove that S is injective. Let $f \in V$, and assume that $Sf = 0$. Then

$$0 = \langle Sf, f \rangle = \sum_{k=1}^m |\langle f, f_k \rangle|^2,$$

which implies that $f = 0$. Now we prove that S is surjective. Since $\{f_k\}_{k=1}^m$ is a frame for V , by corollary 1.1.3, we can say that $\text{span}\{f_k\}_{k=1}^m = V$. So

the pre-frame operator T is surjective.

That is, given any $f \in V$, we can find a $g \in V$ such that $Tg = f$ and in specific we can choose $g \in N_T^\perp = R_{T^*}$ and it follows that $R_S = R_{TT^*} = V$. Thus S is surjective. Therefore S is invertible.

Now each $f \in V$ has the representation

$$\begin{aligned} f &= SS^{-1}f \\ &= TT^*S^{-1}f \\ &= \sum_{k=1}^m \langle S^{-1}f, f_k \rangle f_k. \end{aligned}$$

Since S is self-adjoint, we have

$$f = \sum_{k=1}^m \langle f, S^{-1}f_k \rangle f_k.$$

The second representation is obtained in a similar way by using $f = S^{-1}Sf$.

Now to prove the third result, suppose that $f = \sum_{k=1}^m c_k f_k$. We can write

$$\{c_k\}_{k=1}^m = \{c_k\}_{k=1}^m - \{\langle f, S^{-1}f_k \rangle\}_{k=1}^m + \{\langle f, S^{-1}f_k \rangle\}_{k=1}^m.$$

By the choice of $\{c_k\}_{k=1}^m$, we have

$$\sum_{k=1}^m (c_k - \langle f, S^{-1}f_k \rangle) f_k = 0,$$

i.e, $\{c_k\}_{k=1}^m - \{\langle f, S^{-1}f_k \rangle\}_{k=1}^m \in N_T = R_{T^*}^\perp$; and $\{\langle f, S^{-1}f_k \rangle\}_{k=1}^m = \{\langle S^{-1}f, f_k \rangle\}_{k=1}^m \in R_{T^*}$. Since they belong to two mutually orthogonal sets, we obtain (iii). □

Note 3.1.6. The numbers $\langle f, S^{-1}f_k \rangle$, $k = 1, 2, \dots, m$ are called frame coefficients.

Since $S: V \rightarrow V$ is bijective, the sequence $\{S^{-1}f_k\}_{k=1}^m$ is also a frame by Corollary 1.1.3, called the canonical dual of $\{f_k\}_{k=1}^m$.

Corollary 3.1.7. *Assume that $\{f_k\}_{k=1}^m$ is a basis for V . Then there exists a unique family $\{g_k\}_{k=1}^m$ in V such that*

$$f = \sum_{k=1}^m \langle f, g_k \rangle f_k, \quad \forall f \in V. \quad (3.11)$$

In terms of the frame operator, $\{g_k\}_{k=1}^m = \{S^{-1}f_k\}_{k=1}^m$. Furthermore, $\langle f_j, g_k \rangle = \delta_{j,k}$.

Theorem 3.1.8. *Let $\{f_k\}_{k=1}^m$ be a frame for finite dimensional vector space V . Given $f \in V$, there exist co-efficients $\{d_k\}_{k=1}^m \in \mathbb{C}^m$ such that $f = \sum_{k=1}^m d_k f_k$, and*

$$\sum_{k=1}^m |d_k| = \inf \left\{ \sum_{k=1}^m |c_k| \quad : \quad f = \sum_{k=1}^m c_k f_k \right\}. \quad (3.12)$$

Proof. Fix $f \in V$. There exists a set of co-efficients $\{c_k\}_{k=1}^m$ such that $f = \sum_{k=1}^m c_k f_k$. Let $\sum_{k=1}^m |c_k| = r$. We need to minimize the l^1 norm of the co-efficients.

Let us define two sets M and M' in the following manner:

$$M := \left\{ \{d_k\}_{k=1}^m \in \mathbb{C}^m \quad : \quad |d_k| \leq r, \quad k = 1, \dots, m \right\},$$

$$M' := \left\{ \{d_k\}_{k=1}^m \in M \quad : \quad f = \sum_{k=1}^m d_k f_k \right\}.$$

The function $\phi: M' \rightarrow \mathbb{R}$, defined by $\phi\{d_k\}_{k=1}^m = \sum_{k=1}^m |d_k|$ is continuous by its definition. Since M' is compact and ϕ is continuous on a compact set, it attains its minimum and hence our result.

□

There are some important differences between Theorem 1.1.5 and Theorem 1.1.8. In Theorem 1.1.5 we find the sequence minimizing the l^2 -norm of the coefficients in the expansion of f explicitly. It is unique. On the other

hand, Theorem 1.1.8 only gives the existence of an l^1 -minimizer, and it might not be unique.

Theorem 3.1.9. *Let $\{f_k\}_{k=1}^m$ be a frame for a subspace W of a vector space V . Then the orthogonal projection of V onto W is given by*

$$Pf = \sum_{k=1}^m \langle f, S^{-1}f_k \rangle f_k. \quad (3.13)$$

Proof. Define P as given in (1.13). If $f \in W$, then by theorem 1.1.5,

$$\sum_{k=1}^m \langle f, S^{-1}f_k \rangle f_k = f,$$

$$\text{i.e., } Pf = f \quad \text{for } f \in W.$$

Now since S is a bijection on W , range of S^{-1} is W .

$$\text{i.e., } Pf = 0 \quad \text{for } f \in W^\perp.$$

Hence the result. □

3.2 Pseudo inverses

We know that all matrices do not have an inverse and the matrix which has an inverse is that which is nonsingular. In case no inverse exists, it is convenient to search for "generalized inverses" which can satisfy some of the nice properties of inverses. The right definition of a generalized inverse depends upon the properties we are interested in.

Given an $m \times n$ matrix E , we consider it as a linear mapping of \mathbb{C}^n into \mathbb{C}^m . E is not necessarily injective, but by restricting E to the orthogonal complement of the kernel N_E , we obtain the injective linear mapping,

$$\tilde{E}: N_E^\perp \rightarrow \mathbb{C}^m.$$

Clearly E and \tilde{E} have same range, i.e, $R_E = R_{\tilde{E}}$. So \tilde{E} can be considered as a mapping from N_E^\perp to R_E , which is injective and has an inverse,

$$(\tilde{E})^{-1}: R_E \rightarrow N_E^\perp.$$

Consider \mathbb{C}^m as the direct sum of range of E and its orthogonal complement, i.e, $\mathbb{C}^m = R_E \oplus R_E^\perp$.

Now we can extend $(\tilde{E})^{-1}$ to an operator $E^\dagger: \mathbb{C}^m \rightarrow \mathbb{C}^n$ by defining

$$E^\dagger(y + z) = (\tilde{E})^{-1}y \quad \text{if } y \in R_E, z \in R_E^\perp \quad (3.14)$$

With this definition,

$$EE^\dagger x = x, \quad \forall x \in R_E. \quad (3.15)$$

The operator E^\dagger is called the pseudo-inverse of E . From the definition, we have the following equalities:

$$N_{E^\dagger} = R_E^\perp = N_{E^*}, \quad R_{E^\dagger} = N_E^\perp = R_{E^*} \quad (3.16)$$

Following are the two characterizations of the pseudo-inverse:

Proposition 3.2.1. *Let E be an $m \times n$ matrix. Then*

(i) E^\dagger is the unique $n \times m$ matrix for which EE^\dagger is the orthogonal projection onto R_E and $E^\dagger E$ is the orthogonal projection onto R_{E^\dagger}

(ii) E^\dagger is the unique $n \times m$ matrix for which EE^\dagger and $E^\dagger E$ are self-adjoint and

$$EE^\dagger E = E, \quad E^\dagger EE^\dagger = E^\dagger.$$

Proof. We will prove the proposition in two steps. In first step, we will prove the equivalence between the statements in the proposition. In the next step, we will prove the equivalence between the properties in Proposition and the definition of pseudo-inverse.

Step 1:

Suppose the matrix E^\dagger satisfies (i). i.e, EE^\dagger is the orthogonal projection onto R_E . Then, if $y \in R_E, z \in R_E^\perp$

$$\begin{aligned} EE^\dagger(y+z) &= y \\ \text{i.e, } E^\dagger EE^\dagger(y+z) &= E^\dagger y \\ &= (\tilde{E})^{-1} y \\ &= E^\dagger(y+z). \end{aligned}$$

Similarly we can do the same for the other part. i.e, $EE^\dagger E = E$.
Now suppose the condition (ii) is satisfied.

Step 2: By the definition of pseudo-inverse, we know that,

$$\begin{aligned} \text{If } y \in R_E, \text{ then } EE^\dagger y &= y; \\ \text{If } y \in R_E^\perp = N_{E^\dagger}, \text{ then } EE^\dagger y &= 0. \end{aligned}$$

This proves that EE^\dagger is the orthogonal projection onto R_E . Now

$$\begin{aligned} \text{If } y \in R_{E^\dagger}^\perp = N_E, \text{ then } E^\dagger E y &= y; \\ \text{If } y \in R_{E^\dagger}, y = E^\dagger x \text{ for some } x. & \\ \text{Then, } EE^\dagger y = E^\dagger EE^\dagger x = E^\dagger x - E^\dagger(I - EE^\dagger)x &= E^\dagger x = y. \end{aligned}$$

This proves that $E^\dagger E$ is the orthogonal projection onto R_{E^\dagger} .

We are only left with the proof that if a matrix E^\dagger satisfies conditions (i) and (ii) of the proposition, then it fulfills the requirements in the definition of pseudo-inverse. Note that condition (ii) implies that

$$E^* = (EE^\dagger E)^* = (E^\dagger E)^* E^* = E^\dagger EE^*$$

This in fact shows that,

$$N_E^\perp = R_{E^*} \subseteq R_{E^\dagger}.$$

Now, if $y \in R_E$, then we can find $x \in N_E^\perp \subseteq R_{E^\dagger}$ such that $y = Ex$; thus

$$E^\dagger y = E^\dagger Ex = x = (\tilde{E})^{-1} Ex = (\tilde{E})^{-1} y.$$

Finally, if $y \in R_E^\perp = N_{E^*}$, then by (i), $EE^\dagger z = 0$; using (ii),

$$E^\dagger z = E^\dagger EE^\dagger z = 0.$$

□

Following theorem talks about important minimization problem:

Theorem 3.2.2. *Let E be an $m \times n$ matrix. Given $y \in R_E$, the equation $Ex = y$ has a unique solution of minimal norm, namely $x = E^\dagger y$.*

Proof. We know, by the definition of pseudo-inverse, that $x = E^\dagger y$ is a solution to the equation $Ex = y$. All solutions have the form $x = E^\dagger y + z$, where $z \in N_E$. Since $E^\dagger y \in N_E^\perp$, the norm of the general solution is given by

$$\|f\|^2 = \|E^\dagger y + z\|^2 = \|E^\dagger y\|^2 + \|z\|^2,$$

which is minimal when $z = 0$. □

3.3 Singular value decomposition

For computational purposes it is important to notice that the pseudo-inverse can be found using the singular value decomposition of E which will be discussed in this section.

Lemma 3.3.1. *Let E be an $m \times n$ matrix with rank $r \geq 1$. Then there exist constants $\sigma_1, \sigma_2, \dots, \sigma_r > 0$ and orthonormal bases $\{u_k\}_{k=1}^r$ for R_E and $\{v_k\}_{k=1}^r$ for R_{E^*} such that*

$$Ev_k = \sigma_k u_k, \quad k = 1, 2, \dots, r. \quad (3.17)$$

Proof. Observe that \mathbb{C}^n is a complex vector space and E^*E is a self-adjoint operator which implies that it is a normal operator. Spectral Theorem says that \mathbb{C}^n has an orthonormal basis consisting of eigenvectors of E^*E if and only if E^*E is normal.

Let $\{v_k\}_{k=1}^n$ be the orthonormal basis for \mathbb{C}^n consisting of the eigenvectors

for E^*E . Let $\{\lambda_k\}_{k=1}^n$ denote the corresponding eigenvalues. Note that for each k ,

$$\lambda_k = \lambda_k \|v_k\|^2 = \langle E^* E v_k, v_k \rangle = \|E v_k\|^2 \geq 0.$$

The rank of E is given by

$$r = \dim R_E = \dim R_{E^*}.$$

□

Chapter 4

Wavelet Analysis

Definition 4.0.2 (Continuous Wavelet Transform). *A function $\psi \in L^2(\mathbb{R})$ with $\int_{\mathbb{R}} \psi(x) dx = 0$ is called a wavelet. For every $f \in L^2(\mathbb{R})$, the continuous wavelet transform of it is defined as [3]*

$$T_{\psi}f(a, b) = \langle f, \psi_{a,b} \rangle = \int_{\mathbb{R}} f(x) \bar{\psi}_{a,b}(x) dx, \quad \forall a \in \mathbb{R}^+, \quad b \in \mathbb{R}, \quad (4.1)$$

where $\psi_{a,b}(x) = \frac{1}{\sqrt{a}} \psi\left(\frac{x-b}{a}\right)$. The function ψ is the so called mother wavelet.

The resolution of identity ensures that the reconstruction of f can be made from $\langle f, \psi_{a,b} \rangle$ as follows:

$$f(x) = \int_{\mathbb{R}} \int_{\mathbb{R}} (T_{\psi}f)(a, b) \bar{\psi}_{a,b}(x) \frac{db da}{a^2}. \quad (4.2)$$

4.1 Discrete Wavelet Transform

Under certain restrictions on the mother wavelet ψ , all information about the transformed signal is preserved when the wavelet transform is sampled on certain discrete subsets of the time-frequency plane. More precisely, the values of the continuous transform at these points are the coefficients of a corresponding wavelet basis series expansion.

Now, return to the CWT and consider the case $a = 2^{-j}$, $b = 2^{-j}k$, where $j, k \in \mathbb{Z}$. Then we get

$$\psi_{2^{-j}, 2^{-j}k} = \frac{1}{\sqrt{2^{-j}}} \psi\left(\frac{x - 2^{-j}k}{2^{-j}}\right) = 2^{\frac{j}{2}} \psi(2^{-j}x - k). \quad (4.3)$$

Let $w_{j,k}$ represent the values of the CWT, the wavelet coefficients, at the coordinates $(2^{-j}k, 2^{-j})$ representing a dyadic grid in the time-scale plane. The values correspond to the correlation between f and $\psi_{a,b}$ at specific points (a, b). This sampling keeps enough information to make a perfect reconstruction of the signal possible if some special conditions on the wavelet function are fulfilled. If, in addition, even more conditions on ψ are fulfilled, then it turns out that it is possible to construct a function ψ such that $(\psi_{j,k})_{j,k}$ forms an orthonormal basis. This concept leads to what is called the Discrete Wavelet Transform, (DWT). The reconstruction of f from its coefficient given by an orthonormal wavelet basis is

$$f = \sum_{j,k} w_{j,k} \psi_{j,k}, \quad (4.4)$$

where

$$w_{j,k} = \langle f, \psi_{j,k} \rangle. \quad (4.5)$$

This is a doubly infinite sum over both the time index k and the scale index j . However, the sum can be made finite with little or no error. The case with finitely supported wavelets is clear and for infinitely supported wavelets the main energy should still be concentrated within a certain interval, thus finite summation over k is valid with some approximation. To understand why finite summation over j is valid, with some approximation, we introduce the concept Multiresolution Analysis, (MRA). The MRA, developed by Mallat and Meyer gives the theoretical ground for construction of most wavelets.

Definition 4.1.1 (Multiresolution Analysis). *A multiresolution analysis is a family of closed subspaces $V_j \subset L^2(\mathbb{R})$ with the following properties:*

1. $V_j \subset V_{j+1}, \forall j \in \mathbb{Z}$

2. $f \in V_j \iff f(2\cdot) \in V_{j+1}, \quad \forall j \in \mathbb{Z}$
3. $\overline{\cup_{j \in \mathbb{Z}} V_j} = L^2(\mathbb{R})$
4. $\cap_{j \in \mathbb{Z}} V_j = \{0\}$
5. $\exists \phi \in V_0$ such that $(\phi(x - k))_{k \in \mathbb{Z}}$ is an orthonormal basis for V_0 .

The function ϕ in (5) is the so called scaling function (or sometimes the approximation function). Note that $V_0 = \overline{\text{Span}_k \phi_k}, k \in \mathbb{Z}$, where $\phi_{0,k}(x) = \phi(x - k)$. Except for the assumptions on ϕ due to the MRA, it is usually required that the scaling function should be localized in time. Also, it is common to normalize ϕ and demand $\int_{\mathbb{R}} \phi(x) dx = 1$. Now, the definition of MRA implies

$$\phi(x) = 2 \sum_k h_k \phi(2x - k), \quad (4.6)$$

which is known as the scaling equation. Now, we investigate the detail spaces W_j , where $V_{j+1} = V_j \oplus W_j$. One can prove that there is a function ψ such that $(\psi_{j,k})_k$ is an orthonormal basis of W_j . For instance, $(\psi(\cdot - k))_k$ is an orthonormal basis of W_0 . It also follows that $(\psi_{j,k})_{j,k}$ is an orthonormal basis for $L^2(\mathbb{R})$.

4.2 Wavelet tight frame in 1D

Recall that an orthogonal basis $\{f_k\}_{k=1}^n$ in \mathbb{R}^n satisfies $\sum_{k=1}^n |\langle f, f_k \rangle|^2 = \|f\|^2$ for all $f \in \mathbb{R}^n$ and that $\{f_k\}, k = 1, \dots, n$ is linearly independent. The tight frame is a generalization of orthogonal basis, where the linear independence in the latter is discarded for better flexibility. In particular, a tight frame in \mathbb{R}^n is a set of vectors $\{f_k\}_{k=1}^m$ with $m \geq n$ satisfying

[4]

$$\sum_{k=1}^m |\langle f, f_k \rangle|^2 = \|f\|^2. \quad (4.7)$$

The tight frame analysis operator is defined as

$$W = [f_1, f_2, \dots, f_m]^T,$$

and the synthesis operator is W^T . In other words, $Wf = \{\langle f, f_k \rangle\}_{k=1}^m$ is a vector of the coefficients that are the inner-products of f and f_k , and $W^T c = \sum_{k=1}^m c(i) f_k$ is the synthesis of the coefficients to a signal. The identity (4.7) is equivalent to

$$W^T W = I_n,$$

where I_n is the identity operator from \mathbb{R}^n to \mathbb{R}^n . We call it the perfect reconstruction property.

The wavelet tight frame is a tight frame with the structure deriving from discrete wavelet transform. More precisely, let $h = \{h_i\}_{i=0}^{r-1}$ be a family of filters, where h_0 (lowpass filter), satisfies $\sum_j h_0(j) = 1$, and h_i , $i = 1, \dots, (r-1)$, the so-called high-pass filters, satisfy $\sum_j h_i(j) = 0$. The discrete wavelet transform associated with filters h is defined as follows. Given a signal $x \in \mathbb{R}^n$, we pass it through the filters h_i , $i=0, \dots, r-1$, respectively.

Define

$$W(h) : f \in \mathbb{R}^n \rightarrow \begin{pmatrix} h_0 * f \\ h_1 * f \\ \cdot \\ \cdot \\ h_{r-1} * f \end{pmatrix} \in \mathbb{R}^{rn}. \quad (4.8)$$

where $*$ is the filtering procedure. Then $W(h)$ corresponds to the one-level wavelet transform. To get a multi-level wavelet transform, we need to apply $W(h)$ recursively to the low-pass coefficients that correspond to the low-pass filter h_0 , until a desired level is reached. In order to make the wavelet transform $W(h)$ form a tight frame, the perfect reconstruction property $W(h)^T W(h) = I_n$ should be satisfied, which is finally reduced to certain conditions on the filters h . It is shown that the perfect reconstruction property is equivalent to the following condition:

$$\sum_{i=0}^{r-1} \sum_{n \in \mathbb{Z}} h_i(k+n)h_i(n) = \delta_k, \forall k \in \mathbb{Z}, \quad (4.9)$$

where $\delta_k = 1$ if $k = 0$ and $\delta_k = 0$ otherwise.

An example of wavelet tight frame is the so-called piecewise linear B-spline framelet. The associated filters are

$$h_0 = \frac{1}{4}[1, 2, 1], h_1 = \frac{\sqrt{2}}{4}[1, 0, 1], h_2 = \frac{1}{4}[1, 2, 1]. \quad (4.10)$$

It can be easily checked that the filter $h = \{h_i\}_{i=0}^2$ satisfies (4.7). Consequently, $W(h)$ forms a tight frame. This tight frame has been successfully used in many image reconstruction tasks.

Chapter 5

Computed Tomography in Compressive Sensing Framework

Two major categories of methods exist, analytical reconstruction and iterative reconstruction. Methods based on filtered back projection (FBP) are one type of analytical reconstruction that is currently widely used on clinical CT scanners because of their computational efficiency and numerical stability. Many FBP-based methods have been developed for different generations of CT data-acquisition geometries, from axial parallel- and fan-beam CT in the 1970s and 1980s to current multi- helical CT and cone-beam CT with large area detectors.[?]

5.1 Algebraic Reconstruction Technique (ART)

An entirely different approach for tomographic imaging consists of assuming that the cross section consists of an array of unknowns, and then setting up algebraic equations for the unknowns in terms of the measured projection data which makes the following algebraic system of equations:

$$\sum_{j=1}^N w_{ij} f_j = p_i, i = 1, 2, \dots, M.$$

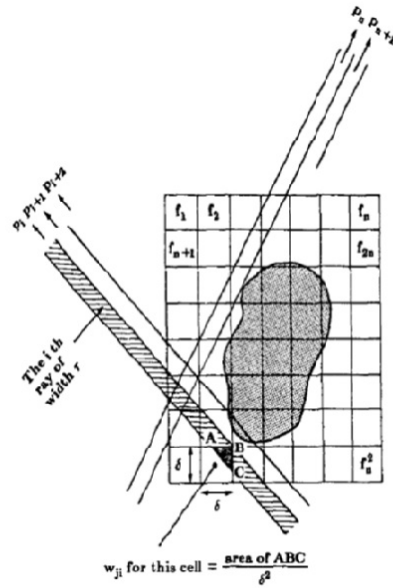


Figure 5.1: ART description.

where M is the total number of rays (in all projections) and w_{ij} is the weighing factor that represents the contribution of the j^{th} cell to the i^{th} ray integral. The factor w_{ij} is equal to the fractional area of the j^{th} image cell intercepted by the i^{th} ray as shown for one of the cells in figure 2. It may be emphasized here that most of the w_{ij} 's are zero since only a small number of cells contribute to any given ray-sum. When put in matrix form above system of equations becomes:

$$p = Af. \quad (5.1)$$

If M and N are small, we may use conventional methods from matrix theory to invert the system of equations. However, in practice N may be as large as 65,000 (for 256 x 256 images), and, in most cases for images of

this size, M will also have the same magnitude. For these values of M and N , the size of the matrix A becomes 65,000 X 65,000, which precludes any possibility of direct matrix inversion. This is precisely the case where CS based methods offer some advantages.

For large values of M and N there exist very attractive iterative methods for solving (1). These are based on the "projection method" as first proposed by Kaczmarz and later elucidated further by Tanabe.

For the computer implementation of this method, we first make an initial guess at the solution. This guess, denoted by $(f_1^{(0)}, f_2^{(0)}, \dots, f_N^{(0)})$, is represented vectorially by $\vec{f}^{(0)}$ in the N -dimensional space. In most cases, we simply assign a value of zero to all the f_i 's. This initial guess is projected on to the hyperplane represented by the first equation in (1) giving $\vec{f}^{(1)}$. $\vec{f}^{(1)}$ is projected on the hyperplane represented by the second equation in (1) to yield $\vec{f}^{(2)}$ and so on. When $\vec{f}^{(i-1)}$ is projected on the hyperplane represented by the i^{th} equation to yield $\vec{f}^{(i)}$. The process can be mathematically described by

$$\vec{f}^{(i)} = \vec{f}^{(i-1)} - \frac{(\vec{f}^{(i-1)} \cdot \vec{w}_i - p_i)}{\vec{w}_i \cdot \vec{w}_i} \vec{w}_i,$$

where $\vec{w}_i = (w_{i1}, w_{i2}, \dots, w_{iN})$, and $\vec{w}_i \cdot \vec{w}_i$ is the dot product of \vec{w}_i with itself.

5.2 1D TV Optimization

Of late, the inherent sparsity present in CT images started attracting the attention of many researchers. In 2006, a compressed sensing (CS) reconstruction algorithm was proposed by Candes et al. They indicated that medical images could be sparsified by taking the gradient transform, and the reconstruction could be improved by solving a constrained minimization problem,

$$\min_f \|f\|_{TV}, \quad s.t. \quad Rf = p \quad (5.2)$$

where R is the Radon transform, p is the projection data and f is the image to be reconstructed. In this section, we first provide general terms and descriptions of TV norm based method in detail. The TV of an image is defined as the l_1 norm of its gradient. For an image f , let $f_{x,y}$ be a pixel value at (x, y) . Then, let the local gradient operator ∇

$$\nabla f_{x,y} = (D_x f_{x,y}, D_y f_{x,y}), \quad (5.3)$$

where D_x and D_y are the discrete differential operators along the x- and y-axes, which are, respectively

$$D_x f_{x,y} = f_{x,y} - f_{x-1,y}, \quad D_y f_{x,y} = f_{x,y} - f_{x,y-1}, \quad (5.4)$$

The position relationship between $f_{x,y}$ and its neighboring pixels is shown in figure (7.1). Then problem equation (5.2) can be rewritten as

$$\min_f \|\vec{\nabla} f\|_{TV}, \quad s.t. \quad Rf = p, \quad (5.5)$$

where $\vec{\nabla} f$ stands for the local gradient operation on every pixel of f and for convenience, we arrange all the results in a single vector. In our-work to solve problem (5.2) (or problem (5.5)) a hybrid SART and TV reconstruction algorithm is used. A steepest descent method is applied to minimize $\|\nabla f\|_1$ and the SART is applied to guarantee the data fidelity.

Let us further expand the calculation of the TV norm of f as

$$\|f\|_{TV} = \|\vec{\nabla} f\|_1 = \sum_{x,y} \|\nabla f_{x,y}\|, \quad (5.6)$$

and usually an L_2 norm will be considered for $\|\nabla f_{x,y}\|$,

$$\|\nabla f_{x,y}\| = \|\nabla f_{x,y}\|_2 = \sqrt{(D_x f_{x,y})^2 + (D_y f_{x,y})^2}. \quad (5.7)$$

It is easy to find out that $\|f\|_{TV}$ is an isotropic expression. Therefore the following conclusion can be derived: an image that is gradient-sparse is also sparse if one calculates a 1D gradient along a certain direction on the image plane. Thus it is possible to deduct a 1D TV minimization problem for CT

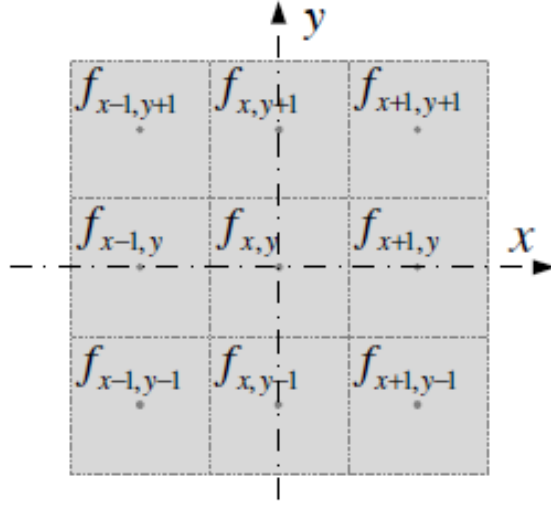


Figure 5.2: Position relationship between $f_{x,y}$ and its neighboring pixels.

reconstruction. Considering the 1D gradient along a radical direction, given a unit vector \vec{e}_α in the plane. one has

$$\nabla_\alpha f_{x,y} = (\nabla f_{x,y} \cdot \vec{e}_\alpha) \vec{e}_\alpha. \quad (5.8)$$

Then the 1D TV minimization problem can be written as

$$\min_f \|\vec{\nabla}_\alpha f\|_1, \quad s.t. \quad Rf = p, \quad (5.9)$$

where the vector sign in $\vec{\nabla}_\alpha f$ is similar as in $\vec{\nabla} f$. The position relationship is shown in figure (7.3). As can be seen from equation (5.9), the minimization objective is no longer the TV norm of image, but the summation of 1D TV of a series of parallel lines. However, such minimization only utilizes the image sparsity along one direction; hence solving such a problem is less effective than the standard 2D TV minimization. To achieve a high performance, more than one direction [?] can be chosen simultaneously. This forms a multi-1D minimization problem.

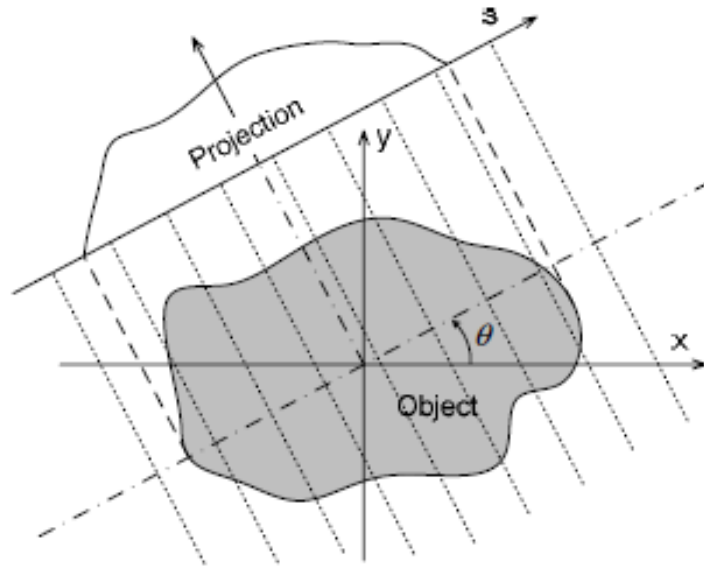


Figure 5.3: Projection geometry.

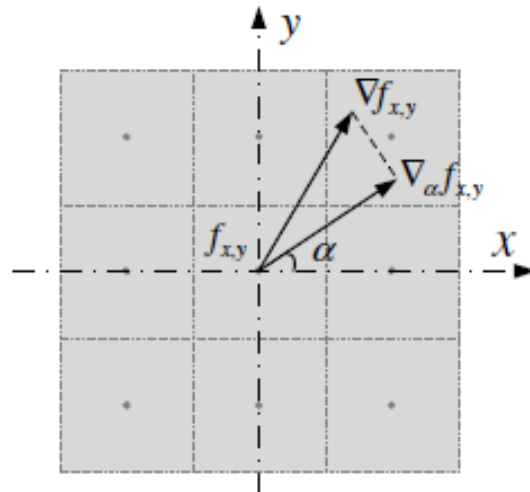


Figure 5.4: Illustration of the calculation of 1D TV.. (Courtesy: Zhiqiang Chen et al. (2013))

Chapter 6

Experimental Result

Error computation by wavelet based OMP for phantom image (64x64)

Threshold	Row-size	Error
10	m	2.4294
	m/2	3.3898
	m/4	5.4835
	m/8	6.4197
7	m	1.9131
	m/2	3.7168
	m/4	5.5573
	m/8	6.9788
0.1	m	0.1052
	m/2	1.5892
	m/4	5.1837
	m/8	7.5819

Error computation by wavelet based OMP for phantom image (32x32)		
Threshold	Row-size	Error
7	m	2.2439
	m/2	2.7996
	m/4	3.9630
	m/8	4.0167
0.1	m	0.4865
	m/2	2.5378
	m/4	3.3686
	m/8	4.2105
0.01	m	0.1671
	m/2	2.1974
	m/4	4.6782
	m/8	6.5679

Error computation by wavelet OMP for phantom image (64x64)		
Threshold	Row-size	Error
7	m	3.8150
	m/2	5.7114
	m/4	8.4808
	m/8	10.6276



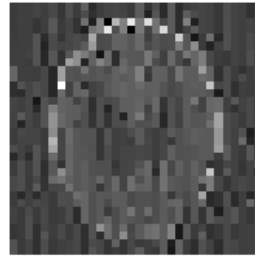
(a) Original Phantom Image(32x32)

th0.1



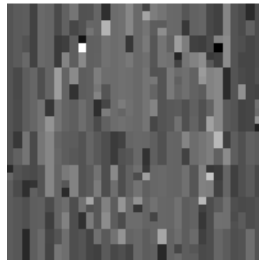
(b) Rows=m

th0.1



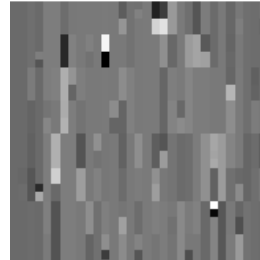
(c) Rows=m/2

th0.1



(d) Rows=m/4

th0.1



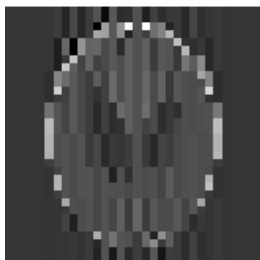
(e) Rows =m/8

Figure 6.1: Reconstruction Phantom Image(32x32) at Threshold=0.1 by Wavelet based OMP



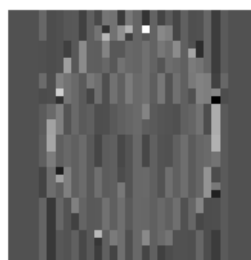
(a) Original Phantom Image(32x32)

th07



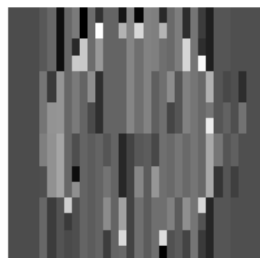
(b) Rows=m

th07



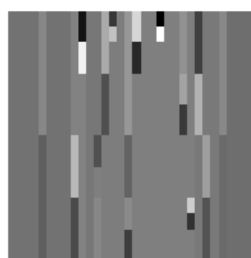
(c) Rows=m/2

th07



(d) Rows=m/4

th07

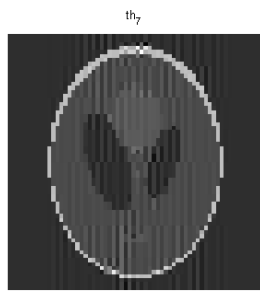


(e) Rows =m/8

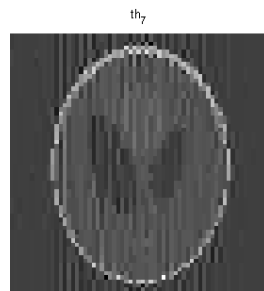
Figure 6.2: Reconstruction Phantom Image(32x32) at Threshold=7 by Wavelet based OMP



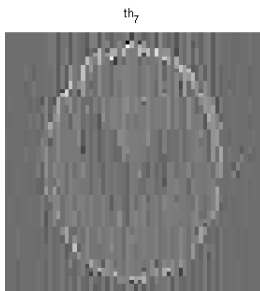
(a) Original Phantom Image(64x64)



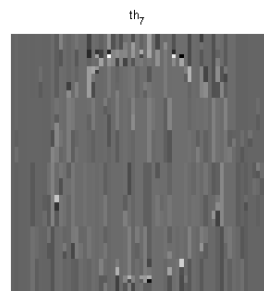
(b) Rows=m



(c) Rows=m/2



(d) Rows=m/4

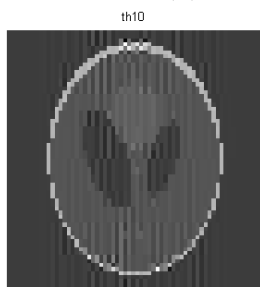


(e) Rows =m/8

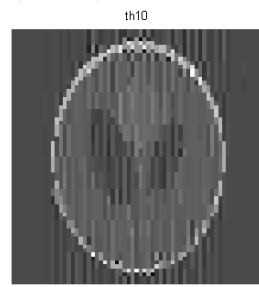
Figure 6.3: Reconstruction Phantom Image(64x64) at Threshold=7 by Wavelet based OMP



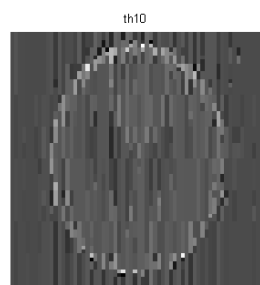
(a) Original Phantom Image(64x64)



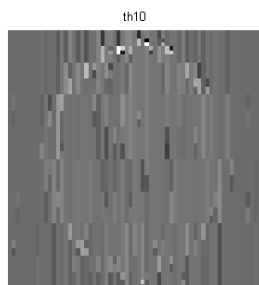
(b) Rows=m



(c) Rows=m/2



(d) Rows=m/4

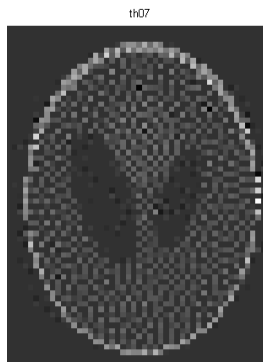


(e) Rows =m/8

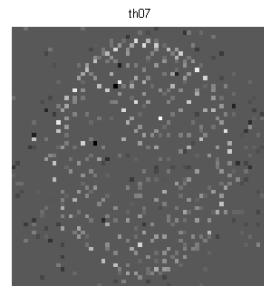
Figure 6.4: Reconstruction Phantom Image(64x64) at Threshold=10 by Wavelet based OMP



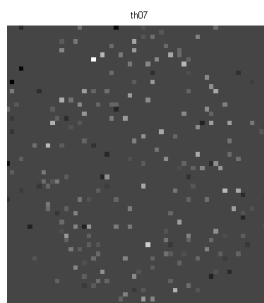
(a) Original Phantom Image(32x32)



(b) Rows=m



(c) Rows=m/4



(d) Rows=m/8

Bibliography

- [1] PETER KUCHMENT, The Radon Transform and Medical Imaging 4,SIAM
- [2] OLE CHRISTENSEN: An Introduction to Frames and Riesz Bases, Springer Science + Business Media, LLC
- [3] Elin Johansson: Wavelet Theory and some of its Applications,
- [4] Weifeng Zhou¹, Jian-Feng Cai and Hao Gao:Adaptive tight frame based medical image reconstruction: a proof-of-concept study for computed tomography,Inverse Problems 29 (2013) 125006 (18pp)
- [5] Zhiqiang Chen, Xin Jin, Liang Li, and GeWang 2013: A limited-angle CT reconstruction method based on anisotropic TV minimization, Phys. Med. Biol., 58, pages 2119–2141 (2013)